*Journal of Non-Newtonian Fluid Mechanics*, 11 (1982) 301–316
Elsevier Scientific Publishing Company, Amsterdam – Printed in The Netherlands



# STEADY PLANAR EXTENSION WITH LUBRICATED DIES *

C.W. MACOSKO, M.A. OCANSEY **

*Chemical Engineering and Materials Science, University of Minnesota, Minneapolis, MN 55455 (U.S.A.)*

and

H.H. WINTER

*Chemical Engineering, University of Massachusetts, Amherst, MA 01003 (U.S.A.)*

Received August 17, 1981; in revised form May 21, 1982)

## Summary

We demonstrate that planar stagnation flow can be achieved using molten polystyrene in a die with walls lubricated by silicone oil. The boundary conditions and flow in the lubrication layer are discussed. Wall pressures drop by nearly an order of magnitude under lubricated conditions. Pressure values were below the accuracy of our transducers. However, both normal stress differences were measured by birefringence and at low extension rate were found in good agreement with the values expected for a Newtonian fluid. Even unlubricated flow gave similar stress differences at the same flow rates, indicating that the shear is confined to a thin layer near the die wall. Tracer pictures confirm this. Extrudate swell was also measured and found to be in reasonable agreement with total recoverable strain predicted from shear measurements.

## 1. Introduction

Measurement of extensional material functions is still relatively undeveloped in comparison to shear rheometry. Great progress has been made in uniaxial extension; however, relatively few results are available in planar or

* Presented at VIIIth Int. Congr. Rheol., Naples, 1980.
** Present address: Exxon Chemical, Inc., Baton Rouge, LA 70821.

0377-0257/82/0000–0000/$02.75 © 1982 Elsevier Scientific Publishing Company

biaxial extension [1,2]. Recently, we have suggested that lubricated stagnation flow dies can be used for generating steady extensional flow [3]. Van Aken and Janeschitz-Kriegl [4,5] used lubricated stagnation flow for generating equal biaxial extension. They recently reported birefringence and total thrust data for polystyrene. Here we report experimental results with a lubricated planar stagnation die using polystyrene melt samples and silicone oil as lubricant. Some of our initial results have already been described [6].

Several investigators [3,7,8] have generated unaxial extensional flow in tapered dies with a lubricated wall. The dies were fed by converging flow from an upstream reservoir of larger cross section. The total strain in these experiments was found to be very small due to unfavorable inlet conditions [3]. A major reason for preferring stagnation flows is to increase this total strain and reach steady state in stresses.

## 2. Dynamics of planar stagnation flow

The kinematics of planar extensional flow at constant density are

$$(\mathbf{v}) = (\dot{\varepsilon}x, -\dot{\varepsilon}y, 0), \tag{1}$$

where $x$, $y$, $z$ are the coordinates in the principal directions shown in Fig. 1. The rate of extension $\dot{\varepsilon}$ is assumed to be constant throughout the fluid and, in the case of steady planar extension, independent of time. Then material elements move along stream surfaces

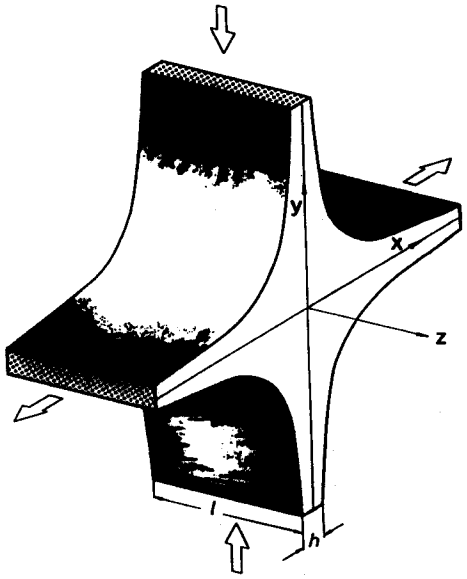


Fig. 1. Planar stagnation flow formed by the impingement of two long rectangular jets; $xy = A$ is the equation for a stream surface; $x_0$, $y_0$ are coordinates at the entrance to the flow.

$$xy = \text{const.} = x_0 y_0 = A. \tag{2}$$

The extension of a material element when moving from $x_0$ to $x$ is

$$\varepsilon = \ln(x/x_0). \tag{3}$$

A material element entering at the symmetry plane, $x = 0$, will be subjected to an infinite strain, while a material element on the outer stream surface, $xy = A$, is stretched the least. The volumeric flow rate between stream surfaces $xy = A$ and $xy = -A$ is proportional to the extension rate,

$$Q_m = 2\dot{\varepsilon} l A, \tag{4}$$

where $l$ is the stream width.

Two normal-stress coefficients or "planar viscosities" can be defined in steady planar extension:

$$\eta_{xy} = (T_{xx} - T_{yy})/\dot{\varepsilon} \tag{5}$$

and

$$\eta_{yz} = (T_{yy} - T_{zz})/\dot{\varepsilon}. \tag{6}$$

A third viscosity can be defined equivalently: $\eta_{xz} = \eta_{xy} + \eta_{yz}$. For a Newtonian fluid with viscosity $\eta_0$ these coefficients become

$$\eta_{xy} = 4\eta_0, \qquad \eta_{yz} = -2\eta_0, \qquad \eta_{xz} = 2\eta_0. \tag{7}$$

If we neglect gravity and inertial effects, the stress on the stream surface has the components [3] (see Fig. 2)

$$T_{nn} = \frac{y^2}{x^2 + y^2}(T_{xx} - T_{yy}) + T_{yy}, \tag{8}$$

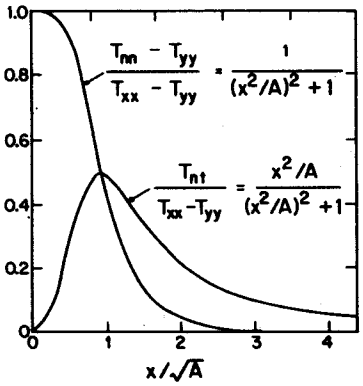


Fig. 2. Normal stress $T_{nn}$ and shear stress $T_{nt}$ at stream surface $xy = A$ of planar extension flow, eqns. (8) and (9). Subscripts n and t refer to an orthonormal coordinate system $(x_n, x_t)$ which is tangent to the stream surface.

$$T_{nt} = \frac{xy}{x^2 + y^2}(T_{xx} - T_{yy}), \tag{9}$$

where the indices t and n indicate the tangent in the flow direction and the normal to the stream surface, respectively. The normal stress difference $T_{xx} - T_{yy}$ is required to be uniform throughout the volume. The boundary conditions for steady planar extensional flow are therefore:

(a) a finite shear stress along the stream surface, having its maximum value at $x = y = \sqrt{A}$ ;

(b) a tension $T_{nn}$ along the stream surface which decreases in the flow direction (assuming uniform $T_{yy}$). Correspondingly,pressure transducers along thestream surface should read increasing pressure values in the flow direction.

In and effort to achieve this ideal planar stagnation flow, the test fluid is pumped through a die with lubricated walls. If the lubricant layer can be made thin, then the die wall can be made to follow a stream surface. Further analysis of the lubricant layer is given in the Appendix. Below we present some experimental observations of the stresses and deformations in planar stagnation flow.

## 3. Experimental

### *3.1. Apparatus*

Figure 3a shows a cross-section of the planar stagnation flow die (die # 1) used for most of the experiments. A material elemtns passing through the die at the stream surface is stretched by $\varepsilon = 3.0$. The stream surface id defined by $xy = A = 69.8$ mm$^2$. Figure 3b shows the die with the top and end melt feed plates removed. The end plate divides the melt stream equally and directs it into two circular channels. The other end plate distributes the lubricant into the four semicircular channels from which it flows through a narrow gap and then is directed down along the die walls. A second die (die #2) of similar dimensions but with windows in each of the end plates was also used for some visualization studies. Ocansey [9] gives more details of the apparatus.

Figure 4 shows the set-up for supplying molten polymer and lubricant to the die. A 1 in. diameter Killion extruder with a maximum output of about 10 kg/h delivered a polystyrene melt to the die.A gear pump (Zenith ZM; $\frac{1}{4}$ hp 1725 rpm motor) metered out the lubricant at 0–2.7 cm$^3$/s. Hydrocarbon oils were found unstable at the high temperatures used but silicone oils worked well (Dow Corning 200 Fluid). A silicone oil with 1 Pa s viscosity worked better than several lubricants with lower viscosities but a systematic study of viscosity influence was not done. Temperature of the lubricant, the

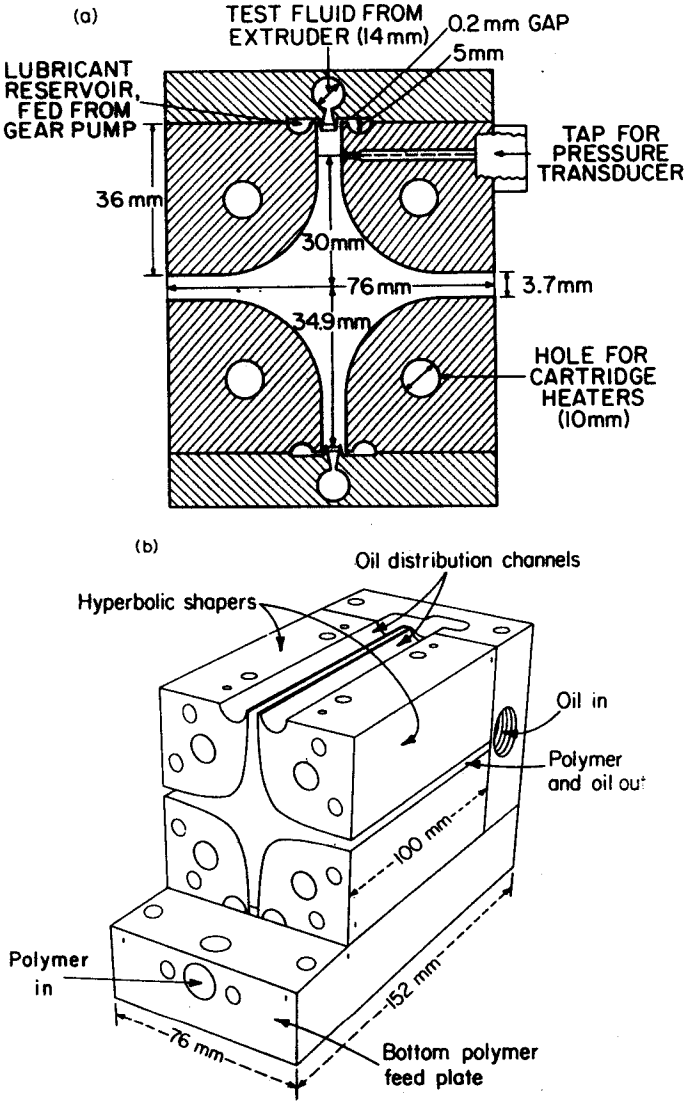


Fig. 3. (a) Cross section of the planar stagnation die, stream width $l = 100$ mm, $x_0 = 2.0$ mm, $y_0 = 34.9$ mm. Pressure tap for measuring $p_1$. (b) Planar stagnation die with the top and end melt feed plates removed.

incoming melt and the die were maintained at $\pm$ 1 K of the test temperature by proportional controllers.

### 3.2. *Materials*

A general purpose polystyrene (Monsanto; Lustrex 101) was used. Its weight average molecular weight was $4.0 \times 10^5$ and polydispersity was 2.0 by

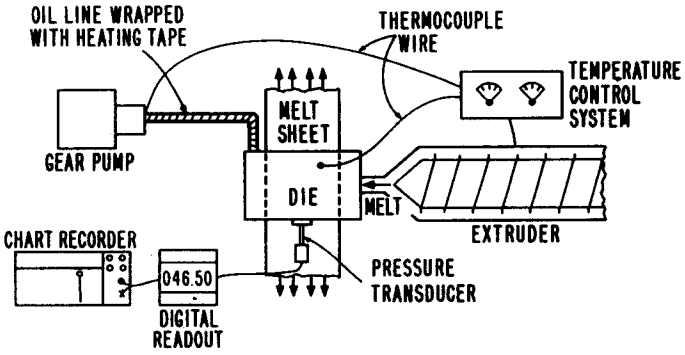


Fig. 4. Arrangement of lubricated stagnation die with extruder for feeding polymer melt, gear pump for the silicone oil lubricant and pressure transducer.

gel permeation chromatography. Its zero shear rate viscosity was $1.7 \times 10^4$ Pa s at 200°C by steady and oscillatory shear measurements in the cone and plate mode of a Rheometrics Mechanical Spectrometer. From steady shear normal stress measurements in the cone and plate, the limiting zero shear rate compliance [10] was determined as

$$J_e^0 = \lim_{\dot{\gamma} \to 0} \frac{T_{11} - T_{22}}{2(T_{12})^2} = 6 \times 10^{-5}\ \text{Pa}^{-1}. \tag{10}$$

Some uniaxial extensional measurements were made using a Rheometrics Extensional Rheometer [11,12]. In both constant rate and constant stress modes, steady state was achieved relatively quickly (at low strain) as has been reported for similar commercial polystyrene samples [12,13].

## 4. Procedure and results

### *4.1. Lubrication procedure*

Unlubricated experiments were first conducted and the pressure at the inlet, $p_1$, recorded. A typical pressure recorded after start up of the extruder is shown in Fig. 5. The steady state value of $9.6 \times 10^4$ Pa compares fairly well to $13.8 \times 10^4$ Pa calculated by approximating the die shape with two wedges and then using Hamel's exact solution for a Newtonian fluid [14].

To achieve lubrication, the die was first taken apart and polymer removed from the test volume. It was then reassembled and heated to the test temperature. The gear pump was started, flooding the die with the lubricant and ensuring that all the walls were covered. Melt was then pumped into the die under the lowest extruder flowrate. When melt was first pumped into an empty die it was not possible to achieve lubrication. Also, it was generally

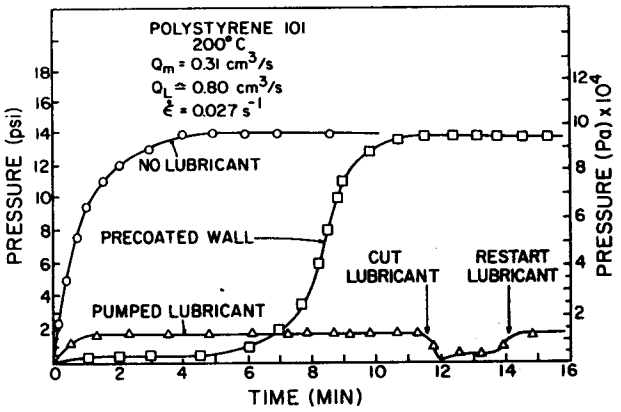


Fig. 5. Typical inlet pressure traces, $p_1$, for three lubrication conditions.

not possible to reestablish lubrication after stopping the experiment.

After lubricated stagnation flow had been established, the extruder flowrate was increased. Timed samples were cut from the die and weighed to determine the flowrate of the melt. This was used to calculate the average extension rates by eqn. (4). A melt density of $10^3$ kg/m$^3$ was used for polystyrene at 200°C.

A typical pressure trace for steady lubricant pumping is also shown in Fig. 5. We see that at the same flow rate with lubrication the pressure is much less than without lubricant. The pressure $p_1$, however, is dependent on the pressure in the lubricant as generated by the gear pump. When the pump is momentarily cut off, the pressure drops considerably to a new steady state which can be maintained for several minutes before lubrication is lost.

This result was checked with another set of experiments performed without pumping the lubricant. A piece saved from the previous experiment was coated with lubricant and inserted into the die. The die and the extruder barrel were then heated up to the test temperature. The extruder was then started up at a known flowrate and the response of the pressure as a function of time was recorded. A typical trace is shown in Fig. 5. At the given flowrate, lubrication is lost after about 6 minutes, but the steady state pressure up to that point agrees with that measured when the gear pump is shut off in the previous run. This is the condition under which pressure data were taken.

Detailed pressure data are not reported here, since the commercial pressure transducers could not accurately measure the low pressures at the wall. Secondly, we were not able to find increasing pressures along the wall of the die (increasing $x$ while $xy = A$) as predicted from eqn. (8). Therefore it was not possible to determine viscosity functions from the pressure data.

Note that the procedure used is different from the one proposed by

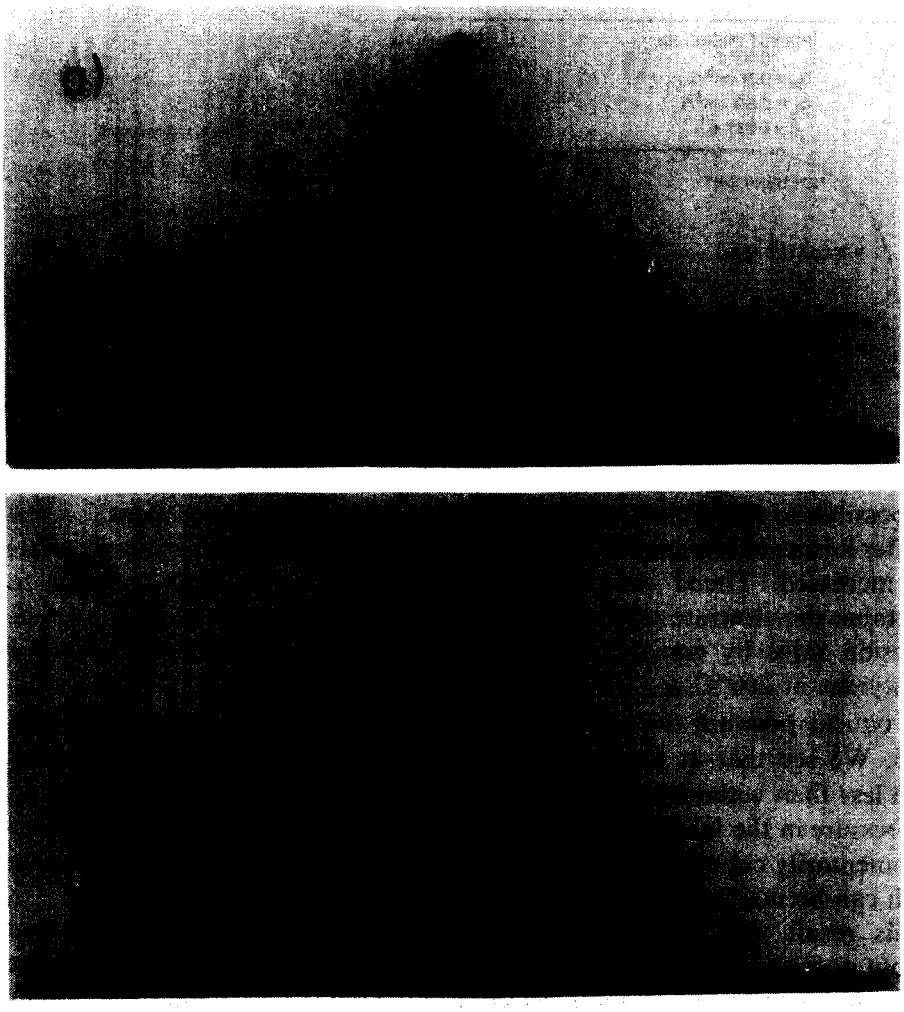

Fig. 6. Tracer studies under (a) lubricated and (b) unlubricated conditions. $Q_m = 0.14$ cm$^3$/s $Q_L \cong 0.2$ cm$^3$/s, 200°C. Note the stagnation line at the center of the die. Dashed lines were added to photographs to define the edge of the transparent samples.

Everage and Ballman [8] who continued to pump lubricant while taking their pressure measurements and then subtract off the pump pressure. We found this procedure quite inaccurate in our case.

In general we found it difficult to achieve lubrication. Temperature control across the die length was critical. The lubricant must be preheated or it will cool off the end of the die causing non-uniform flow and loss of lubrication. If the lubricant flow rate is too high it can cause unstable flow: pockets of lubricant form at the wall and waves appear on the extrudate surface. We were able to achieve good lubrication with a flow rate of 1.5–3

times the polymer flowrate. As mentioned above, we were not able to achieve lubrication at the maximum extruder output. The major cause of this was backing up to polymer melt into the oil distribution lines. This could be improved by narrowing the lubricant feed gap and possibly by using a higher viscosity oil. A more fundamental problem may be the lubrication of the end plates.

Some qualitative observations of the velocity field in the die were also made. A solid polystyrene piece from a previous run was removed from the cold die. Holes 1.3 mm diameter were drilled in the $y$ direction near the entrance plane and black rods of polystyrene were inserted. The test piece was coated with lubricant, replaced into the die, heated and then fed with more melt at a low flow rate for about 2 minutes. The piece was again cooled, removed, and machined to reveal the tracer. A precoated and an unlubricated sample are shown in Fig. 6. For ideal stagnation flow the tracer line should remain horizontal. For the lubricated experiment, the $y$ coordinate varies from center to wall by 12%. This may be due to distortions of the tracer upon heating and cooling in addition to shear stresses in a non-ideal lubricant layer. The tracer showed that there was slip at the wall. For the unlubricated experiment the tracer makes a streak along the wall demonstrating the no-slip boundary conditions. However, it is remarkable that the velocity profile is so flat near the center of the unlubricated flow. When the dimensions of the two test pieces in Fig. 6 are compared they agree to within 0.2 mm except near the center where the piece from the lubricated die is 0.5 mm narrower. These results indicated that under our normal operating conditions the lubricant layer was quite thin.

### *4.2. Flow birefringence*

The stress was measured through the anisotropy of birefringence. Janeschitz-Kriegl and co-workers have shown that the stress optical law holds for polystyrene melts over a very wide range of deformation rate [4,15,16]. The optical system shown in Fig. 7 consists of a tungsten light source, a lens, a slit, a polarizer, a wedge-shaped glass window 6 mm wide

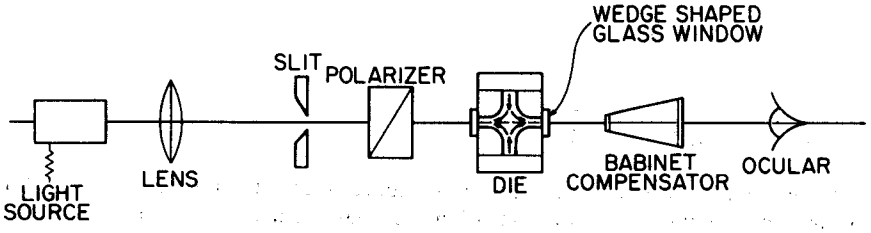


Fig. 7. Schematic of line birefringence optical measurement system.

across each exit plane of the die and a Babinet compensator. The slit gives a beam of light in the $x$ direction about 2 mm thick. With this arrangement, the birefringence $\Delta n_{yz}$ was measured. For planar extension the principal stresses are aligned with the coordinate direction, and the birefringence is proportional to the principal stress difference

$$\Delta n_{yz} = C(T_{yy} - T_{zz}), \tag{11}$$

where $C$ is the stress optical coefficient, $C = 4.0 \times 10^{-9}$ m$^2$/N, for polystyrene [16]. Using the second die with windows in the end plates and the same optical system we were able to measure the birefringence in the $x$, $y$ plane

$$\Delta n_{xy} = C(T_{xx} - T_{yy}). \tag{12}$$

The amount of birefringence in the $y$, $z$ plane was measured under lubricated and unlubricated conditions and compared in Fig. 8. The agreement between them is surprisingly good. This says that the state of stress near the center of the die, along streamlines near $y = 0$, is independent of wall conditions. This same result can be inferred from tracers in Fig. 6. Using eqns. (11) and (6) the planar viscosity was determined and plotted in Fig. 9. Again we see good agreement between data obtained with lubricated and unlubricated flow.

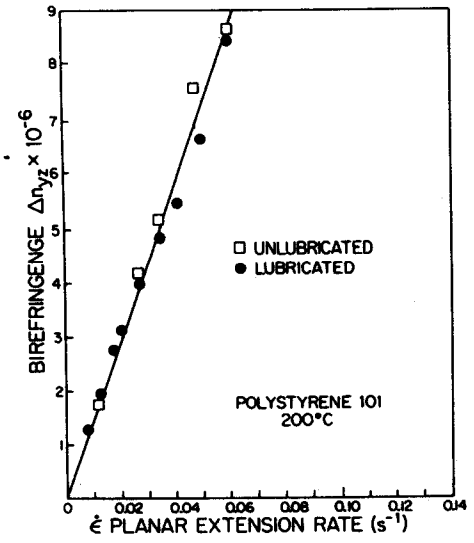


Fig. 8. Birefringence difference in the $y$, $z$ plane as a function of extension rate at 200°C for both lubricated and unlubricated flow. Extension rate was calculated as $\dot{\epsilon} = Q/2x_0t_0l$ for both cases.

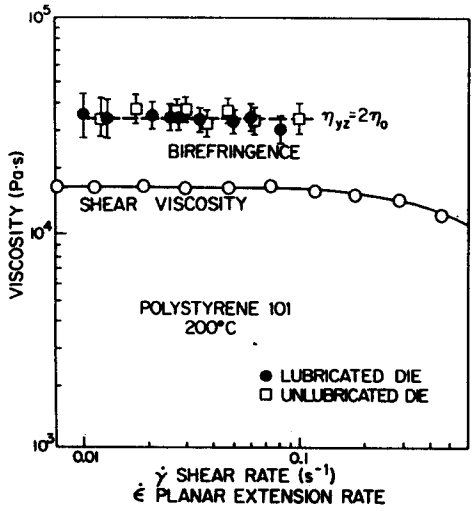


Fig. 9. Extensional viscosity results from birefringence measurements with die #1 of Fig. 8 compared to shear at 200°C.

Figure 10 shows birefringence data taken with the second die which has windows in the end plates. The first normal stress difference was calculated using eqn. (12). The agreement with $4\eta_0$ is good. Full field birefringence measurements with this die show a large region of uniform stress around the stagnation line [9]. Further birefringence studies are in progress.

### *4.3. Extrudate swell*

Since ideal lubricated planar stagnation flow is homogeneous, the thickness of the extrudate should measure recoverable strain. The polystyrene melt was extruded from the die under lubricated conditions onto a lubri-

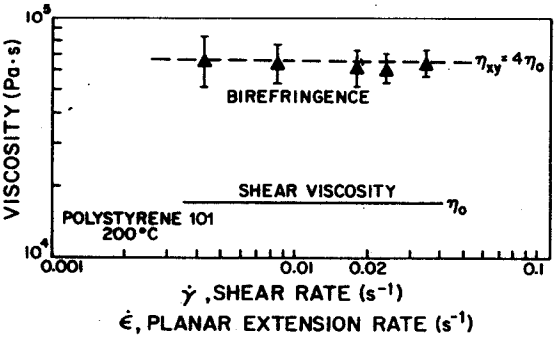


Fig. 10. Extensional viscosity results from birefringence measurements with die #2 in the $x, y$ plane, unlubricated flow compared to shear data at 200°C.

cated sheet of metal. The extrudate was cut into 5–10 cm lengths and allowed to swell to equilibrium in a silicone oil bath of the same temperature as the die for about one hour. The final thickness divided by die gap opening is plotted in Fig. 11.

The total recoverable strain for these low deformation rates can be calculated from $J_e^0$

$$J_e^0 = \varepsilon_r/(T_{xx} - T_{yy}) = \varepsilon_r/4\eta_0\dot{\varepsilon}. \tag{13}$$

Using the values for $J_e^0$ and $\eta_0$ reported above we obtain

$$\varepsilon_r = H/H_0 - 1 \doteq 4.1\,\dot{\varepsilon}. \tag{14}$$

This result is plotted as the solid line in Fig. 11. The agreement is reasonably good. There is very little extrudate swell because the deformation rates are so low.

## 5. Conclusion

We have demonstrated that lubricated stagnation flow can be achieved experimentally and can be used to obtain extensional material functions. Lubrication was shown in the large reduction in pressure for the same flow rate, and by the tracer profiles.

Everage and Ballman's [8] problem of low total strain and thus difficulty in achieving steady state in the stresses is solved here by using stagnation flow in which the total strain along the central streamline is infinite and nowhere is less than 3. In stagnation dies, the minimum total strain can reasily be increased by changing the curvature.

The approximate analysis of the lubricant layer demonstrates that steady

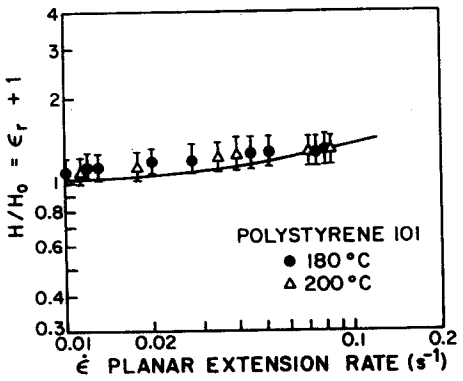


Fig. 11. Equilibrium extrudate swell after lubricated die flow for polystyrene 101 at 200°C and 180°C. The solid line is calculated from the recoverable strain predicted from $J_e^0$ and $\eta_0$, eqns. (13), (14).

planar extension cannot be achieved in the entire sample. An optimal design of the lubricant layer will give a large region of steady planar extension around the stagnation line. The decision on optimal lubrication conditions will only be possible after an analysis of the complete two phase flow of the sample together with the lubricant. This analysis is in progress.

The potential advantage of lubricated flows over "pulling type" experiments [11–13] is that they can be used at higher extension rates and on lower viscosity fluids. In this study we believe that we were limited to lower rates by our extruder feed and by back up in the lubricant feed slots. This is being rectified with a new die. In our earlier paper [3] we demonstrated that lubrication can be achieved for a sample fluid of very low viscosity. Further work is in progress in this direction.

Flow birefringence was found to be a sensitive measure of normal stress differences in stagnation flows. A remarkable result of our work is that even without lubrication the stresses near the central strain planes or around the stagnation line are very similar to those expected for steady planar extensional flow.

## Appendix: lubricant layer

An approximate technique is used to analyze the kinematics and the stress in the thin lubricant film between the sample fluid and the solid wall. Possible velocity distributions are sketched in Fig. A1. The layer thickness $\delta(x)$ is small. Therefore, curvature can be neglected in the analysis. The high lubricant flow rates $Q_L$ needed in the experiments suggest that pressure flow was important for the kinematics, i.e. the velocity should be as sketched on the right hand side of Fig. A1. Velocity and stress are most conveniently

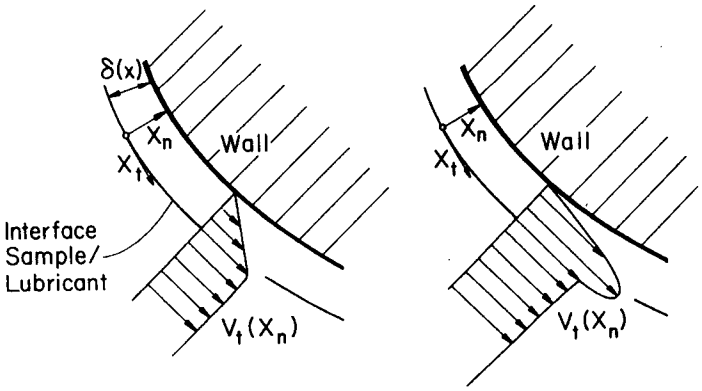


Fig. A1. Sketch of lubricant layer on a curved die wall. Velocity distribution in lubricant layer: drag flow (left side) as compared to a superposition of drag and pressure flow (right side).

described in a local coordinate system ($x_t$, $x_n$) with its origin at the fluid/fluid interface $xy = A$.

The equation of motion for an incompressible Newtonian fluid becomes

$$0 = -\frac{\partial p}{\partial x_t} + \mu \frac{\partial^2 v_t}{\partial x_n^2}, \tag{15}$$

where $\mu$ is the viscosity of the lubricant. Inertia, gravity, and velocity gradients in tangent direction are neglected. The boundary conditions of the velocity field (assuming no slip) are

$$v_t(0) = v_i,\ v_t(\delta) = 0, \tag{16}$$

where $v_i$ is the velocity at the interface. The pressure in the lubricant layer, $p$, is just equal to the negative of the normal stress at the interface, $(T_{nn})_i$:

$$p = -(T_{nn})_i. \tag{17}$$

The pressure gradient can be assumed to be constant across the film. Equation (15) is integrated to get the velocity distribution

$$v_t(x_n) = v_i\left(1 - \frac{x_n}{\delta}\right) + \frac{\partial (T_{nn})_i}{\partial x_t} \frac{x_n \delta}{2\mu}\left(1 - \frac{x_n}{\delta}\right) \tag{18}$$

as sketched in Fig. A1. The shear stress in the lubricated layer at the interface

$$(T_{nt})_i = \mu\left(\frac{\partial v_t}{\partial x_n}\right)_i = -\frac{\mu v_i}{\delta} + \frac{\partial (T_{nn})_i}{\partial x_t} \frac{\delta}{2} \tag{19}$$

can be positive or negative, depending on the contribution of the pressure gradient in the tangent direction. The criterion for a vanishing shear stress at the interface is

$$\frac{\partial (T_{nn})_i}{\partial x_t} \frac{\delta^2}{\mu v_i} = \frac{1}{2}.$$

The thickness of the lubricant layer is determined by the lubricant flowrate

$$Q_L = v_i \frac{\delta l}{2} + \frac{\partial (T_{nn})_i}{\partial x_t} \frac{\delta^3 l}{12\mu} \tag{20}$$

and by the boundary condition $v_i$ and $(T_{nn})_i$. In steady lubrication, the flow rate $Q_L$ is constant along the lubricant film (assuming $l = \text{const.}$) while $Q_L$ for a precoated sample (see Section 4.1) changes in space and time.

Note that $v_i$ and $(T_{nn})_i$ are not known yet. They should be determined by an analysis of the entire two phase flow. We are, however, interested in answering a very specific equation: which lubricant layer kinematics are best for achieving steady planar extension in the sample? The boundary condi-

tions at the fluid/fluid interface required to give steady planar extension are

$$v_i = \dot{\varepsilon}\left(x^2 + A^2/x^2\right)^{1/2} \tag{21}$$

for the velocity and the stress components $T_{nn}$ and $T_{nt}$ of eqn. (8) and eqn. (9). The stress distribution along the interface is shown in Fig. 2. It is important to note that the shear stress is equal to zero at small $x$ and at large $x$, but a finite shear stress is required at intermediate $x$-values.

*Negligible pressure flow*

In a very thin fluid layer, the velocity contribution due to the pressure gradient is negligible compared to the drag contribution (left side of Fig. A1). The condition for such a thin layer is (see eqn. (18))

$$\left|\frac{\partial p}{\partial x_t}\frac{\delta^2}{\mu v_i}\right| \ll 1. \tag{22}$$

The *shear* stress at the interface, eqn. (19), becomes independent of the *normal* stress distribution along the interface:

$$(T_{nt})_i = -\mu v_i/\delta. \tag{23}$$

In steady lubrication, the flow rate $Q_L$ is constant and the layer thickness depends just on the velocity $v_i$

$$\delta = 2Q_L/lv_i. \tag{24}$$

The shear stress at the interface then becomes

$$(T_{nt})_i = -\frac{\mu l}{2Q_L}v_i^2. \tag{25}$$

A special case of this boundary condition (for Newtonian fluids on both sides of the interface) has been suggested by Joseph [17].

In our experiment we want to achieve a velocity at the interface, $v_i$, and a shear stress at the interface, $(T_{nt})_i$, which would give steady planar extension, see eqn. (21) and eqn. (9). The desired velocity $v_i$ gives a *negative* shear stress (from eqn. (25))

$$(T_{nt})_i = -\frac{\mu l}{2Q_L}v_i^2 = \frac{\mu\dot{\varepsilon}Q_m}{4AQ_L}\left(x^2 + A^2/x^2\right), \tag{26}$$

while the desired shear stress $(T_{nt})_i$ is *positive* (from eqn. (9))

$$(T_{nt})_i = \frac{A}{x^2 + A^2/x^2}\left(T_{xx} - T_{yy}\right). \tag{27}$$

It therefore can be concluded that a very thin lubricant layer is not

favourable for achieving the desired boundary condition. It comes closest if the shear stress is made small, i.e. if the coefficient $\mu\dot{\varepsilon}Q_m/AQ_L$ is made small. This might be the reason why we only could establish lubrication with a substantial pressure flow component in the lubricant film.

## Acknowledgements

This work was supported by grants from the Mobil Oil corporation and the National Science Foundation, CME-79-07045. Silicone oil was donated by the dow Corning Corporation. We are grateful to Professor Janeschitz-Kriegl for suggesting birefringence measurements through the exit slits of the die.

## References

1 J.M. Dealy, J. Non-Newt. Fluid Mech., 4 (1978) 9.
2 C.J.S. Petrie, Elongational Flows, Pitman, London, 1979.
3 H.H. Winter, C.W. Macosko and K.E. Bennett, Rheol. Acta, 18 (1979) 323.
4 J.A. Van Aken and H. Janeschitz-Kriegl, Rheol. Acta, 19 (1980) 744.
5 J.A. Van Aken and H. Janeschitz-Kriegl, Rheol. Acta, 20 (1981) 419.
6 C.W. Macosko, M.A. Ocansey and H.H. Winter, in: G. Astarita and G. Nicolais (Eds.), Proc. VIIIth Int. Congr. Rheol., Naples, Plenum Press, 1980, Vol. 3, p. 723–728.
7 M.T. Shaw, J. Appl. Polym. Sci., 19 (1975) 2811.
8 A.E. Everage and R.L. Ballman, Nature, 273 (1978) 213.
9 M.A. Ocansey, M.S. Thesis, Department of Chemical Engineering and Materials Science, University of Minnesota, 1981.
10 W.W. Graessley, Adv. Polym. Sci., 16 (1974) 1.
11 H. Münstedt, J. Rheol., 23 (1979) 421.
12 V. AuYeung and C.W. Macosko, in: G. Astarita and G. Nicolais (Eds.), Proc. VIIIth Int. Congr. Rheol., Naples, Plenum Press, 1980, Vol. 3, p. 717–722.
13 H. Münstedt, J. Rheol., 24 (1980) 847.
14 G.K. Batchelor, An Introduction to Fluid Dynamics, Cambridge Press, 1967, pp. 294–300.
15 H. Janeschitz-Kriegl, Adv. Polym. Sci., 6 (1969) 170.
16 F.H. Gortemaker, Doctoral Thesis, TH Delft, 1976.
17 D.D. Joseph, Phys. Fluids, 23 (1980) 2356.